JACS
JOURNAL OF THE AMERICAN CHEMICAL SOCIETY
Communication
pubs.acs.org/JACS

Immobilizing Metal Nanoparticles to Metal–Organic Frameworks with Size and Location Control for Optimizing Catalytic Performance

Qi-Long Zhu,[†] Jun Li,[†,‡] and Qiang Xu*[,†,‡]

[†]National Institute of Advanced Industrial Science and Technology (AIST), Ikeda, Osaka 563-8577, Japan
[‡]Graduate School of Engineering, Kobe University, Nada Ku, Kobe, Hyogo, Japan

Supporting Information

ABSTRACT: AuNi alloy nanoparticles were successfully immobilized to MIL-101 with size and location control for the first time by double solvents method (DSM) combined with a liquid-phase concentration-controlled reduction strategy. When an overwhelming reduction approach was employed, the uniform 3D distribution of the ultrafine AuNi nanoparticles (NPs) encapsulated in the pores of MIL-101 was achieved, as demonstrated by TEM and electron tomographic measurements, which brings light to new opportunities in the fabrication of ultrafine non-noble metal-based NPs throughout the interior pores of MOFs. The ultrafine AuNi alloy NPs inside the mesoporous MIL-101 exerted exceedingly high activity for hydrogen generation from the catalytic hydrolysis of ammonia borane.

Over the past decade, noble metal nanocatalysts have been extensively investigated and exhibited a wide range of potential applications in the fields of energy conversion and storage, environmental remediation, drug research and chemical production.[1] However, the noble catalysts are too expensive to be widely applied in practical applications. To improve the catalytic performance and minimize the usage of noble metals, the synthesis of non-noble metal-based nanocatalysts is an important topic in heterogeneous catalysis.[2] Alloying a parent metal with a second metal offers numerous opportunities for modulating the electronic structures of catalysts and optimizing their catalytic performance.[2]

Metal–organic frameworks (MOFs) synthesized by assembling metal ions with organic ligands have recently emerged as a new class of porous materials for their amenability to design as well as fine-tunable and uniform pore structures.[3] Their distinct characteristics make them very promising for a variety of applications, including gas storage and separation, sensing, optics, drug delivery, and catalysis.[4] Recently, by serving as unique host matrices, the potential applications of MOFs can be extended further by encapsulating metal nanoparticles (MNPs) within the frameworks.[5] The development of this type of composite materials to elicit enhanced properties is of current interest.

General synthetic methods to embed MNPs in a MOF matrix entail the impregnation of metal precursors with various techniques, such as chemical vapor deposition, solution infiltration, and solid grinding, followed by reduction of the metal precursors to metal atoms.[5,6] MOFs have been utilized as supports for MNPs since they provide powerful confinement effect to limit the growth of MNPs; however, the precursor compounds and products can actually diffuse out through the pores of the host to form the MNPs with aggregation on the external surface of MOFs. To circumvent the drawbacks, great efforts have been made. Recently, we developed a double solvent method which could greatly minimize the deposition of metal precursors on the outer surface.[7] When the noble metal precursors are loaded, they can be treated by the hydrogen and plasma reduction methods under relatively moderate conditions which are suited perfectly for the preparation of noble NPs hosted inside the MOFs,[7,8] but not for non-noble metal-based NPs because of contradictions between the high reduction temperatures of non-noble metals and the low thermal stabilities of MOFs. Therefore, a general and facile method that can easily control the nucleation and growth of MNPs, especially non-noble metal-based NPs, with high uniformity only inside the pores of MOF is still imperative.

Herein, we exploit a liquid-phase concentration-controlled reduction (CCR) strategy for the first time to control the size and location of the AuNi NPs during reduction of the Au^{3+} and Ni^{2+} precursors which are introduced into the pores of MOF by using the double solvents method (Figure 1). When an overwhelming reduction (OWR) approach with a high-concentration reductant solution is employed, ultrafine AuNi alloy NPs are successfully encapsulated into the MOF nanopores without aggregation on the external surface. In contrast, serious agglomeration of MNPs can occur if a

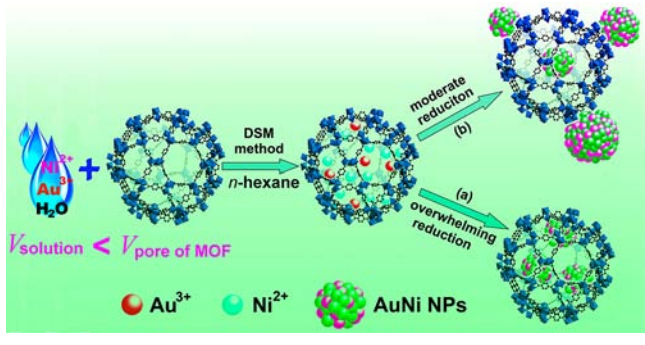

Figure 1. Schematic representation of immobilization of the AuNi nanoparticles by the MIL-101 matrix using the DSM combined with a liquid-phase CCR strategy.

Received: April 4, 2013
Published: June 27, 2013

   dx.doi.org/10.1021/ja403330m | J. Am. Chem. Soc. 2013, 135, 10210–10213

moderate reduction (MR) approach is chosen. The highly dispersed AuNi NPs in the MOF pores exhibit excellent catalytic performance in hydrolytic dehydrogenation of ammonia borane, one of the most attractive candidates for chemical hydrogen storage.[9]

MIL-101, a chromium-based MOF with molecular formula $Cr_3F(H_2O)_2O[(O_2C)C_6H_4(CO_2)]_3{\cdot}nH_2O$ (where n = ~25), was selected as a host matrix in this work to encapsulate metallic particles not only because of its incredibly large pore size (2.9 to 3.4 nm) and high specific surface area (Langmuir surface area reaches 5900 m^2/g) but also because of its long-term stablity in water and air atmospheres.[10] The pore windows with diameters of ~1.2 and 1.6 nm are big enough for the precursor compounds $HAuCl_4$ and $NiCl_2$ to diffuse into the pores, within which nucleation can take place to form the AuNi alloy NPs. The impregnation of metal precursors was conducted by using double solvents method in order to avoid the deposition of the precursors on the outer surface of MOF.[7] Because of the large inner surface area of MIL-101 with hydrophilic character derived from the metal-cluster based trimeric building block,[4j] the small amount of aqueous precursor solution, with a volume slightly less than the pore volume of the adsorbent, was readily incorporated into the pores of dehydrated MIL-101, which was suspended in a large amount of dry *n*-hexane, by capillary force. Since the inner surface area of MIL-101 is much larger than the outer surface area, the small amount of aqueous precursor solution can go inside the hydrophilic pore, and the deposition of metal precursors on the outer surface can be minimized. After loading the precursors and drying the metal precursor/MOF composite, an OWR approach with a high-concentration $NaBH_4$ solution was carried out for avoiding MNPs aggregation on external surfaces of MIL-101 framework, which is based on the assumption that when the metal precursors deposited in the pores of MOF can be reduced completely by a pore-volume amount of $NaBH_4$ solution that can be incorporated into the pores by capillary force, the aggregation of MNPs on the external surface will be avoided utmostly. Otherwise, when a low-concentration $NaBH_4$ solution was used, the reduction of the precursor inside the pores can not be completed, and a part of the precursors would be redissolved and diffuse out of the pores, resulting in the aggregation of MNPs on the outer surface of MOF. Thus, the control of size and location of MNPs can be achieved by using the CCR strategy, i.e., controlling the amount of the reductant in a certain volume of solution equal to the pore volume of MOF.

For preparing MNPs immobilized by MIL-101, activated MIL-101 (200 mg), which possesses a pore volume of 2.11 $cm^3\ g^{-1}$ as determined by N_2 sorption isotherm, was suspended in *n*-hexance (40 mL), to which an aqueous metal precursor solution (0.36 mL) was added dropwise under vigorous stirring. After careful filtration, the synthesized samples were dehydrated at 150 °C, followed by reduction with various concentrations of $NaBH_4$. The uniform MNPs throughout the interior pores of MIL-101 were achieved as the concentration of the aqueous $NaBH_4$ solution was increased to 0.6 M, which therefore was chosen as the critical concentration for the OWR approach. The catalytic activities for hydrolysis of ammonia borane were tested for the prepared samples.[9] Among the catalysts of AuNi@MIL-101 obtained by reduction with 0.6 M aqueous $NaBH_4$ solution, the catalyst with the Au/Ni atomic ratio of 7:93 exhibited the highest activity (vide infra), and therefore $Au_{0.07}Ni_{0.93}$@MIL-101 was chosen as the model catalyst to explore the effect of the reductant concentration on the size and location of the MNPs with the CCR strategy. The resultant nanocomposites obtained by reduction using aqueous $NaBH_4$ solutions of 0.6, 0.4, and 0.2 M are denoted as AuNi@MIL-101_a–c, respectively.

When a high-concentration $NaBH_4$ solution (0.6 M) is used, an OWR takes place to the precursors incorporated in the pores of MIL-101 (Figure 1), resulting in the formation of highly dispersed AuNi alloy NPs with average size of 1.8 ± 0.2 nm encapsulated within the pores of MIL-101 without deposition of the NPs on the external surface, which has been confirmed by the TEM, high-annular dark-field scanning TEM (HAADF-STEM), energy-dispersive X-ray spectroscopy (EDX) analyses and electron tomographic reconstruction (Figures 2a,b, S6 and S7 and a movie for AuNi@MIL-101_a).[11] The two kinds of mesoporous cavities of MIL-101 are large enough to accommodate the small MNPs. These TEM images showed no large particle aggregation, and the electron tomographic reconstruction definitely demonstrated the uniform 3D distribution of monodispersed AuNi NPs throughout the interior cavities of MIL-101 crystals. However, under MR conditions (Figure 1), agglomeration of larger MNPs on the external surface of MIL-101 was observed. In 0.4 M $NaBH_4$ solution, AuNi@MIL-101_b with MNPs of 2.0–5.0 nm was obtained (Figure 2c), while in 0.2 M $NaBH_4$ solution, AuNi@MIL-101_c was formed with most of the MNPs >5.0 nm (Figure 2d). These results indicate that, below the critical concentration of 0.6 M, the reductant in the solution within a volume equal to the pore volume of MOF is not enough to completely reduce the loaded metal precursors, and a part of the metal precursors incorporated within the pores redissolve into the solution and diffuse out of the pores, resulting in the agglomeration of MNPs on the external surface of MOF; the further the reductant concentration selected strays from the critical level, the more severe MNP agglomeration occurs. Consequently, the strategy employed here demonstrates that the combination of the double solvents method and the OWR approach can facilely and effectively control the capsulation of the MNPs into the pores of MIL-101, which can be easily

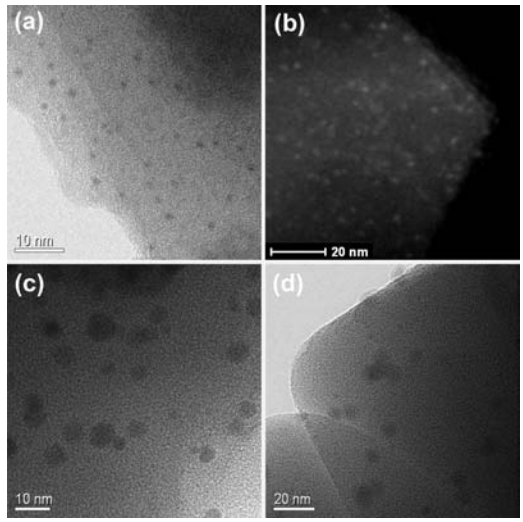

Figure 2. (a) TEM and (b) HAADF-STEM images of AuNi@MIL-101_a; and TEM images of (c) AuNi@MIL-101_b and (d) AuNi@MIL-101_c.

dx.doi.org/10.1021/ja403330m | J. Am. Chem. Soc. 2013, 135, 10210–10213

expanded to the other systems with different metal precursors and MOF matrices possessing hydrophilic pores.[4]

After the impregnation and reduction processes, there is no loss of the crystallinity in powder X-ray diffraction (PXRD) patterns for Au@MIL-101, Ni@MIL-101, and AuNi@MIL-101_a–c, which are similar to the simulated pattern of MIL-101 reported by Férey et al,[10] indicating that the integrity of the MIL-101 framework is maintained (Figures S2 and S3). Moreover, no diffractions were detected for MNPs in M@MIL-101 obtained by reduction via the OWR approach, indicating the formation of very small MNPs. As the size of MNPs increases, the diffractions for the AuNi alloy phases between the characteristic peaks of Au(111) and Ni(111) were observable for the AuNi@MIL-101_b and AuNi@MIL-101_c samples.[11,12] The appreciable decreases in the surface areas and the pore volumes of M@MIL-101 indicate that the pores of the host frameworks are occupied by dispersed MNPs and/or blocked by the MNPs located on surface (Figure S4).[11] The X-ray photoelectron spectroscopic (XPS) investigation of AuNi@MIL-101_a at the Au 4f and Ni 2p levels exhibits that metallic Au and Ni peak intensities changed synchronously during the Ar etching, indicating the homogeneity of the AuNi alloy particles (Figure S5).[11]

It is well-known that ammonia borane (NH_3BH_3, AB) is a promising material for chemical hydrogen storage,[9] from which hydrogen can be released through hydrolysis.[13] In this work, AB hydrolysis is employed for evaluating the catalytic activities of the M@MIL-101 catalysts. Reaction was initiated by introducing aqueous AB solution into the reaction flask containing the as-synthesized M@MIL-101 catalysts with vigorous shaking at room temperature. H_2 generated from the AB hydrolysis was collected in the buret, with which the H_2 volume was monitored. Figures 3 and S11 show the H_2

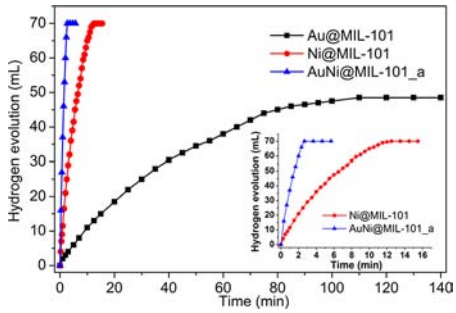

Figure 3. Plots of time vs volume of hydrogen generated from AB (1 mmol in 5 mL water) hydrolysis at room temperature catalyzed by the Au@MIL-101, Ni@MIL-101, and AuNi@MIL-101_a catalysts (50 mg, (Au+Ni)/AB (molar ratio) = 0.017).

generation from aqueous AB in the presence of M@MIL-101 prepared by reduction using 0.6 M $NaBH_4$ with various Au/Ni compositions.[11] It is revealed that the AuNi@MIL-101 catalysts are more active for the hydrolysis of AB than the monometallic counterparts, exhibiting synergistic effect between Au and Ni.[2] Under our evaluation conditions, the AuNi@MIL-101 with the Au/Ni atomic ratio of 7:93 is the most active, in which the AB hydrolysis reaction is completed in 2.67 min with a 70 mL H_2 release, corresponding to H_2/AB = 3 ((Au + Ni)/AB = 0.017 in molar ratio), giving a turnover frequency (TOF) value of 66.2 $mol_{H_2}·mol_{cat}·min^{-1}$. This value is much higher than those of the most active non-noble metal-based catalysts for this reaction reported so far and even higher than those of most Pt, Rh and Ru-related catalysts.[9e,13] Reasonably, the small sizes of surfactant-free AuNi NPs within MIL-101 and synergistic effect between Au and Ni account for the observed high catalytic activity. It is found that the productivity of H_2 over the AuNi@MIL-101_a catalyst almost remained unchanged after five runs, indicating the high durability in AB hydrolysis (Figure S12). Since the degenerative performance can be recovered totally after catalyst recycling, the slight activity drop should be attributed to the increase in concentration of metaborate (BO_2^-) and the viscosity of the solution during the AB hydrolysis. Once metaborate generated during the reaction was removed from solution, the catalyst exhibited its original catalytic activity (Figure S12).[11] PXRD (Figure S14a,b) and TEM (Figures S15a,b) measurements of AuNi@MIL-101_a after catalysis showed no significant change in the morphologies of AuNi NPs with retention of the MIL-101 framework.[11] Uniform distribution of AuNi alloy NPs without aggregation after catalysis confirms the advantage of the confinement effect of the MOF matrix.

It has been known that the catalytic activity generally increases with the decrease in MNP size, as smaller MNPs have higher surface areas available for reactants.[14] Thus, the effect of the size and location of the MNPs on its AB hydrolysis kinetics was further evaluated by using AuNi@MIL-101_a–c, which were obtained by using the CCR reduction strategy. Figure 4

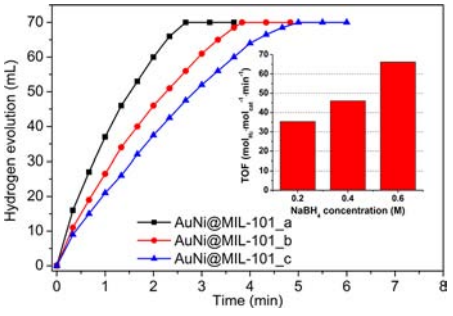

Figure 4. Plots of time vs volume of hydrogen generated from AB (1 mmol in 5 mL water) hydrolysis at room temperature catalyzed by the AuNi@MIL-101_a–c catalysts (50 mg, (Au+Ni)/AB (molar ratio) = 0.017) prepared by reduction in $NaBH_4$ solution with different concentrations. Inset: the corresponding TOF values of the catalysts.

shows the plots of time vs volume of H_2 generated during AB hydrolysis catalyzed by AuNi@MIL-101_a–c with different particle sizes and locations. Comparing with the AuNi NPs in AuNi@MIL-101_a, the AuNi NPs in AuNi@MIL-101_b and AuNi@MIL-101_c exhibit larger sizes with different degrees of agglomeration on the external surface of MIL-101 crystals. Accordingly, their significant decreases in the TOF values from 66.2 to 46.0 and 35.3 $mol_{H_2}·mol_{cat}·min^{-1}$, respectively, and in the initial dehydrogenation rates indicate that the catalytic activity is severely decreased with the increase of MNPs size (Figures 4 inset and S10). Furthermore, AuNi@MIL-101_c features much lower durability in AB hydrolysis than that of AuNi@MIL-101_a, which may be attributed to the lack of the pore confinement effect of MIL-101 to protect the MNPs from agglomeration (Figures S13, S15c,d).[11]

In summary, we have developed a facile and effective approach via a liquid-phase CCR strategy in combination with the DSM for the first time to control the size and location of the MOF-immobilized metal NPs, especially the non-noble metal-based NPs, which are difficult to be obtained by H_2

dx.doi.org/10.1021/ja403330m | J. Am. Chem. Soc. 2013, 135, 10210–10213

reduction at a moderate temperature where MOFs can remain stable. When an OWR approach is employed, the incorporation of ultrafine MNPs within the pores of MOFs without agglomeration of the MNPs on the external surface of host framework is easily achieved. We have used this approach to fabricate ultrafine AuNi alloy NPs inside the mesoporous MIL-101, which could serve as a high-performance catalyst for future development of ammonia borane into a practical hydrogen storage materials for clean energy applications. The present results open up new avenues for developing high-performance heterogeneous catalysts by using porous MOFs as hosts for ultrafine metal NPs, especially non-noble metal-based NPs.

■ ASSOCIATED CONTENT

Supporting Information

Experimental procedures; PXRD, BET, XPS, TEM, EDX for catalysts; results of catalytic AB hydrolysis; durability and stability results of catalysts. This material is available free of charge via the Internet at http://pubs.acs.org.

■ AUTHOR INFORMATION

Corresponding Author

q.xu@aist.go.jp

Notes

The authors declare no competing financial interest.

■ ACKNOWLEDGMENTS

The authors are thankful to the reviewers for valuable suggestions, Dr. Takeyuki Uchida and Dr. Tomoki Akita for TEM measurements and AIST and METI for financial support.

■ REFERENCES

(1) (a) Scott, R. W.; Wilson, O. M.; Oh, S.-K.; Kenik, E. A.; Crooks, R. M. *J. Am. Chem. Soc.* **2004**, *126*, 15583. (b) Guo, Y.-G.; Hu, J.-S.; Wan, L.-J. *Adv. Mater.* **2008**, *20*, 2878. (c) Zhang, H.; Jin, M.; Xia, Y. *Chem. Soc. Rev.* **2012**, *41*, 8035. (d) Hong, X.; Wang, D.; Cai, S.; Rong, H.; Li, Y. *J. Am. Chem. Soc.* **2012**, *134*, 18165.

(2) (a) Bashyam, R.; Zelenay, P. *Nature* **2006**, *443*, 63. (b) Morozan, A.; Jousselme, B.; Palacin, S. *Energy Environ. Sci.* **2011**, *4*, 1238. (c) Jiang, H.-L.; Xu, Q. *J. Mater. Chem.* **2011**, *21*, 13705. (d) Singh, A. K.; Xu, Q. *ChemCatChem* **2013**, *5*, 652.

(3) (a) Eddaoudi, M.; Kim, J.; Rosi, N.; Vodak, D.; Wachter, J.; O'Keeffe, M.; Yaghi, O. M. *Science* **2002**, *295*, 469. (b) Zhang, J.-P.; Huang, X.-C.; Chen, X.-M. *Chem. Soc. Rev.* **2009**, *38*, 2385. (c) Férey, G.; Serre, C. *Chem. Soc. Rev.* **2009**, *38*, 1380. (d) Yuan, D.; Zhao, D.; Sun, D.; Zhou, H.-C. *Angew. Chem., Int. Ed.* **2010**, *49*, 5357. (e) Chen, B.; Xiang, S.; Qian, G. *Acc. Chem. Res.* **2010**, *43*, 1115. (f) Wu, T.; Wang, L.; Bu, X.; Chau, V.; Feng, P. *J. Am. Chem. Soc.* **2012**, *134*, 4517.

(4) (a) Ghosh, S. K.; Bureekaew, S.; Kitagawa, S. *Angew. Chem., Int. Ed.* **2008**, *47*, 3403. (b) Ma, S.; Zhou, H.-C. *J. Am. Chem. Soc.* **2006**, *128*, 11734. (c) Ma, L.; Jin, A.; Xie, Z.; Lin, W. *Angew. Chem., Int. Ed.* **2009**, *48*, 9905. (d) Lee, J.; Farha, O. K.; Roberts, J.; Scheidt, K. A.; Nguyen, S. T.; Hupp, J. T. *Chem. Soc. Rev.* **2009**, *38*, 1450. (e) He, Y.; Xiang, S.; Chen, B. *J. Am. Chem. Soc.* **2011**, *133*, 14570. (f) Motoyama, S.; Makiura, R.; Sakata, O.; Kitagawa, H. *J. Am. Chem. Soc.* **2011**, *133*, 5640. (g) Akiyama, G.; Matsuda, R.; Sato, H.; Takata, M.; Kitagawa, S. *Adv. Mater.* **2011**, *23*, 3294. (h) Shigematsu, A.; Yamada, T.; Kitagawa, H. *J. Am. Chem. Soc.* **2012**, *134*, 13145. (i) Wanderley, M. M.; Wang, C.; Wu, C.-D.; Lin, W. *J. Am. Chem. Soc.* **2012**, *134*, 9050. (j) Küsgens, P.; Rose, M.; Senkovska, I.; Fröde, H.; Henschel, A.; Siegle, S.; Kaskel, S. *Microporous Mesoporous Mater.* **2009**, *120*, 325.

(5) (a) Cheon, Y. E.; Suh, M. P. *Chem.—Eur. J.* **2008**, *14*, 3961. (b) Park, Y. K.; Choi, S. B.; Nam, H. J.; Jung, D.; Ahn, H. C.; Choi, K.; Furukawa, H.; Kim, J. *Chem. Commun.* **2010**, *46*, 3086. (c) Lu, G.; Li, S.; Guo, Z.; Farha, O. K.; Hauser, B. G.; Qi, X.; Wang, Y.; Wang, X.; Han, S.; Liu, X.; DuChene, J. S.; Zhang, H.; Zhang, Q.; Chen, X.; Ma, J.; Loo, S. C. J.; Wei, W. D.; Yang, Y.; Hupp, J. T.; Huo, F. *Nat. Chem.* **2012**, *4*, 310. (d) Dhakshinamoorthy, A.; Garcia, H. *Chem. Soc. Rev.* **2012**, *41*, 5262. (e) Wang, C.; deKrafft, K. E.; Lin, W. *J. Am. Chem. Soc.* **2012**, *134*, 7211. (f) Moon, H. R.; Lim, D.-W.; Suh, M. P. *Chem. Soc. Rev.* **2013**, *42*, 1807. (g) Li, S.-L.; Xu, Q. *Energy Environ. Sci.* **2013**, *6*, 1656.

(6) (a) Hermes, S.; Schröter, M.-K.; Schmid, R.; Khodeir, L.; Muhler, M.; Tissler, A.; Fischer, R. W.; Fischer, R. A. *Angew. Chem., Int. Ed.* **2005**, *44*, 6237. (b) Proch, S.; Herrmannsdörfer, J.; Kempe, R.; Kern, C.; Jess, A.; Seyfarth, L.; Senker, J. *Chem.—Eur. J.* **2008**, *14*, 8204. (c) Jiang, H.-L.; Akita, T.; Ishida, T.; Haruta, M.; Xu, Q. *J. Am. Chem. Soc.* **2011**, *133*, 1304. (d) Gu, X.; Lu, Z.-H.; Jiang, H.-L.; Akita, T.; Xu, Q. *J. Am. Chem. Soc.* **2011**, *133*, 11822.

(7) Aijaz, A.; Karkamkar, A.; Choi, Y. J.; Tsumori, N.; Rönnebro, E.; Autrey, T.; Shioyama, H.; Xu, Q. *J. Am. Chem. Soc.* **2012**, *134*, 13926.

(8) Zou, J.-J.; Zhang, Y.-p.; Liu, C.-J. *Langmuir* **2006**, *22*, 11388.

(9) (a) Gutowska, A.; Li, L.; Shin, Y.; Wang, C. M.; Li, X. S.; Linehan, J. C.; Smith, R. S.; Kay, B. D.; Schmid, B.; Shaw, W.; Gutowski, M.; Autrey, T. *Angew. Chem., Int. Ed.* **2005**, *44*, 3578. (b) Keaton, R. J.; Blacquiere, J. M.; Baker, R. T. *J. Am. Chem. Soc.* **2007**, *129*, 1844. (c) Kim, S.-K.; Han, W.-S.; Kim, T.-J.; Kim, T.-Y.; Nam, S. W.; Mitoraj, M.; Piekos, L..; Michalak, A.; Hwang, S. J.; Kang, S. O. *J. Am. Chem. Soc.* **2010**, *132*, 9954. (d) Kim, S.-K.; Kim, T.-J.; Kim, T.-Y.; Lee, G.; Park, J. T.; Nam, S. W.; Kang, S. O. *Chem. Commun.* **2012**, *48*, 2021. (e) Yadav, M.; Xu, Q. *Energy Environ. Sci.* **2012**, *5*, 9698−9725.

(10) Férey, G.; Mellot-Draznieks, C.; Serre, C.; Millange, F.; Dutour, J.; Surblé, S.; Margiolaki, I. *Science* **2005**, *309*, 2040.

(11) See the Supporting Information.

(12) Zhou, S.; Yin, H.; Schwartz, V.; Wu, Z.; Mullins, D.; Eichhorn, B.; Overbury, S. H.; Dai, S. *ChemPhysChem* **2008**, *9*, 2475.

(13) (a) Yan, J.-M.; Zhang, X.-B.; Han, S.; Shioyama, H.; Xu, Q. *Angew. Chem., Int. Ed.* **2008**, *47*, 2287. (b) Metin, Ö.; Ö zkar, S.; Sun, S. *Nano Res.* **2010**, *3*, 676. (c) Yan, J.-M.; Zhang, X.-B.; Akita, T.; Haruta, M.; Xu, Q. *J. Am. Chem. Soc.* **2010**, *132*, 5326. (d) Sanyal, U.; Demirci, U. B.; Jagirdar, B. R.; Miele, P. *ChemSusChem* **2011**, *4*, 1731. (e) Li, P. Z.; Aijaz, A.; Xu, Q. *Angew. Chem., Int. Ed.* **2012**, *51*, 6753.

(14) (a) Tsunoyama, H.; Sakurai, H.; Negishi, Y.; Tsukuda, T. *J. Am. Chem. Soc.* **2005**, *127*, 9374. (b) Liu, H.; Liu, Y.; Li, Y.; Tang, Z.; Jiang, H. *J. Phys. Chem. C* **2010**, *114*, 13362.